Available online at www.sciencedirect.com
SCIENCE DIRECT
Solid State Communications 137 (2006) 512–516
solid state communications
www.elsevier.com/locate/ssc

Effect of SnO_2 coating on the magnetic properties of nanocrystalline $CuFe_2O_4$

R. Kalai Selvan [a,b,*], C.O. Augustin [a], C. Sanjeeviraja [b], D. Prabhakaran [c]

[a] Central Electrochemical Research Institute, Karaikudi 630 006, India
[b] Department of Physics, Alagappa University, Karaikudi 630 003, India
[c] Clarendon Laboratory, Department of Physics, Oxford University, Oxford OX1 3PU, UK

Received 6 August 2005; received in revised form 8 November 2005; accepted 4 December 2005 by A. Pinczuk
Available online 4 January 2006

Abstract

Nanocrystalline $CuFe_2O_4$ and $CuFe_2O_4/xSnO_2$ nanocomposites ($x=0$, 1, 5 wt%) have been successfully synthesized by one-pot reaction of urea–nitrate combustion method. The transmission electron microscope study reveals that the particle size of the as synthesized $CuFe_2O_4$ and $CuFe_2O_4$/5 wt%SnO_2 are 10 and 20 nm, respectively. The SnO_2 coating on the nanocrystalline $CuFe_2O_4$ was confirmed from HRTEM studies. The resultant products were sintered at 1100 °C and characterized by XRD and SQUID for compound formation and magnetic studies, respectively. The X-ray diffraction pattern shows the well-defined sharp peak that confirms the phase pure compound formation of tetragonal $CuFe_2O_4$. The zero field cooled (ZFC) and field cooled (FC) magnetization was performed using SQUID magnetometer from 2 to 350 K and the magnetic hysteresis measurement was carried out to study the magnetic properties of nanocomposites.

PACS: 61.10.−I; 75.50Gg; 75.50.Pp; 75.60.Ej

Keywords: A. Spinel ferrites; C. X-ray diffraction; D. SQUID magnetometer; E. HRTEM

1. Introduction

Nanocomposites have recently gained considerable interest because of the possibilities of getting unique properties compared to their individual counter parts [1]. Due to their smaller size, these nanocomposites have potential applications in magnetic recording media, information storage devices, magneto optical devices, bio-medical fields and also catalytic anodes for high temperature applications [2,3]. The $CuFe_2O_4$ has an inverse spinel structure, where eight Cu^{2+} ions occupy octahedral (B) sites and 16 Fe^{3+} ions share the octahedral (B) and tetrahedral (A) sites. The magnetic moment of the above system mainly depends upon the uncompensated Cu^{2+} ions, which may due to the cancellation of antiparallel spins of the Fe^{3+} ions in tetrahedral and octohedral sites.

Due to the enhancement of emerging properties for novel applications, the magnetic ferrites are embedded in a non-magnetic oxide matrix [4]. Several researchers have studied the structural, electrical, magnetic properties of individual ferrites like $CuFe_2O_4$ [5], $NiFe_2O_4$ [6], $ZnFe_2O_4$ [7], $CoFe_2O_4$ [8], $MgFe_2O_4$ [9], and their composites like, $NiFe_2O_4/SiO_2$ [10], $NiFe_2O_4/SnO_2$ [11], $CoFe_2O_4/SiO_2$ [12], $ZnFe_2O_4/TiO_2$ [13], $ZnFe_2O_4/SiO_2$ [14] and $CdFe_2O_4/SiO_2$ [15]. The structural, magnetic and electrical properties of the ferrites mainly depend on the method of synthesis, starting materials chosen and sintering temperature. Methods available for preparing the nanomaterials and their composites are combustion synthesis [16], sol–gel method [17], hydrothermal process [18], citrate-gel method [19], reverse micelle technique [20] and sonochemical method [21]. Hence, considering the importance of ferrite nanocomposites as electrode materials for the replacement of carbon anodes in electrochemical systems [22] an attempt to synthesise and to understand the structural and magnetic properties of $CuFe_2O_4/SnO_2$ nanocomposites have been highlighted in this communication, using the techniques of XRD, TEM, HRTEM, and SQUID.

* Corresponding author. Address: EPM Division, Central Electrochemical Research Institute, CECRI Nagar, Karaikudi 630 006, India. Tel.: +91 4565 227550; fax: +91 4565 227779.
E-mail address: selvankram@rediffmail.com (R.K. Selvan).

0038-1098/$ - see front matter © 2005 Published by Elsevier Ltd.
doi:10.1016/j.ssc.2005.12.018

2. Experimental

The nanocomposites of $CuFe_2O_4/SnO_2$ ($x=0$, 1, 5 wt%) have been prepared by using novel combustion synthesis method. The experimental procedure and the thermo dynamical calculations of parent $CuFe_2O_4$ and $CuFe_2O_4/SnO_2$ composites are already explained elsewhere [23,24]. The stoichiometric quantities of starting compounds like $Cu(NO_3)_2\cdot 6H_2O$, $Fe(NO_3)_3\cdot 9H_2O$, $SnCl_4$, HNO_3, $CO(NH_2)_2$ were dissolved in 100 ml distilled water. The mixed nitrate–urea solution was heated at 110 °C, with uniform stirring and evaporated the excess water to form a highly viscous gel denoted as precursors. The gel was heated at 300 °C continuously, get ignited with an evolution of large number of gaseous products, resulting the desired nanocomposite in the form of foamy powder. The powder was then pressed at a pressure of 3.5 tons/cm^2 into 1 and 2.5 cm diameter pellets under identical conditions. The pellets were sintered at 1100 °C for 5 h. The crystalline phases of the prepared powders were identified by powder X-ray diffraction technique using Cu K_α radiation ($\alpha=1.5405$ Å). The particle morphology of all the samples was determined by transmission electron microscopy (TEM; JEOL-JEM 100SX microscope) at an accelerating voltage of 200 kV. The TEM specimens were prepared by placing a drop of the sample suspension on a carbon-coated copper grid (400 mesh, Electron Microscopy Sciences) and allowing them to dry in air. High-resolution TEM (HRTEM) images were taken using a JEOL-3010 with 300 kV accelerating voltage. A conventional monochrome CCD camera, with resolution of 768×512 pixels, was used to digitalize the images. The digital images were processed with the digital micrograph software package (Gatan, Inc., Pleasanton, CA, USA). The effects of temperature and applied magnetic field on magnetization have been carried out using superconducting quantum interference device (SQUID) quantum design.

3. Results and discussion

3.1. Structural properties

The X-ray powder diffraction patterns of the combustion synthesised $CuFe_2O_4/SnO_2$ nanocomposites are presented in Fig. 1. It shows the presence of sharp well-defined peaks corresponding to the planes (220), (311), (400) and (440), indicating the spinel structure of $CuFe_2O_4$ without any impure phase. The lattice constant values confirmed that the pristine $CuFe_2O_4$ is a tetragonal structure with the lattice parameters of $a=8.2740$ Å and $c=8.4814$ Å, which is perfectly match with the standard data [PDF No. 6-545]. From the Debye–Sherror formula, the average particle size has been calculated to be 30 nm, which is larger than the observed TEM values due to high temperature sintering. Interestingly, no significant change was observed in the 1 wt% SnO_2 coated samples. On the other hand, at higher concentration of 5 wt% SnO_2 an extra peak of (110) and (101) corresponding to SnO_2 also emerges. The X-ray lattice parameters (Table 1) are also changed an indication of phase transition from tetragonal to cubic due to

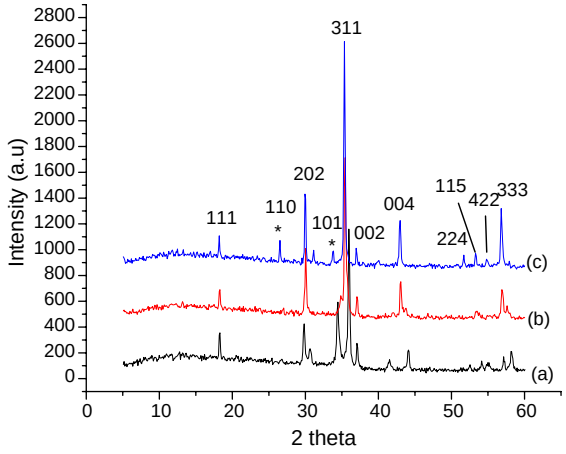

Fig. 1. XRD patterns of $CuFe_2O_4$ (a), $CuFe_2O_4$/1 wt% SnO_2 (b), $CuFe_2O_4$/5 wt% SnO_2.

the 5 wt% added SnO_2 that originates from the difference in ionic radii.

Figs. 2 and 3 show the TEM and HRTEM images of as synthesised nanocrystalline $CuFe_2O_4$ and $CuFe_2O_4/SnO_2$ nanocomposites. Both the samples exhibited the presence of 10–20 nm sized particles individually. The particles are regular and uniform in size. The HRTEM images of $CuFe_2O_4$ confirmed the well-defined lattice fringes with a definite 'd' value of 2.51 Å, which corresponds to the prominent plane of (311) for copper ferrite. The SnO_2 layer coating over the ferrite material is confirmed from the HRTEM image (Fig. 3). It also confirms the composite behaviour of spinel (113) with a 'd' value of 2.63 Å and layered SnO_2 (110) with a 'd' value of 3.35 Å, which are structurally integrated and leads to the structural compatibility and the stability of the composites [25].

3.2. Magnetic properties

The magnetic measurements of $CuFe_2O_4$ and its composites were carried out by SQUID magnetometer. Fig. 4(a)–(c) shows the ZFC and FC curves of nanocrystalline $CuFe_2O_4$, its composites of $CuFe_2O_4$/1 wt% SnO_2 and $CuFe_2O_4$/5 wt% SnO_2, respectively. For ZFC magnetization measurements, the sample was first cooled down to 2 K without applied magnetic field and then the magnetization was measured from 2 to 350 K in the applied magnetic field of 1000 Oe. At ZFC condition the magnetic moments of the particles are randomly oriented due to the Brownian motion, after the applying field the dipole moments of the particles reorient along the field direction generates the net magnetization. For the field-cooled

Table 1
XRD parameters

Sample	Lattice parameters	
	a (Å)	c (Å)
$CuFe_2O_4$	8.2740	8.4814
$CuFe_2O_4$ + 1 wt% SnO_2	8.3904	8.4189
$CuFe_2O_4$ + 5 wt% SnO_2	8.4125	–

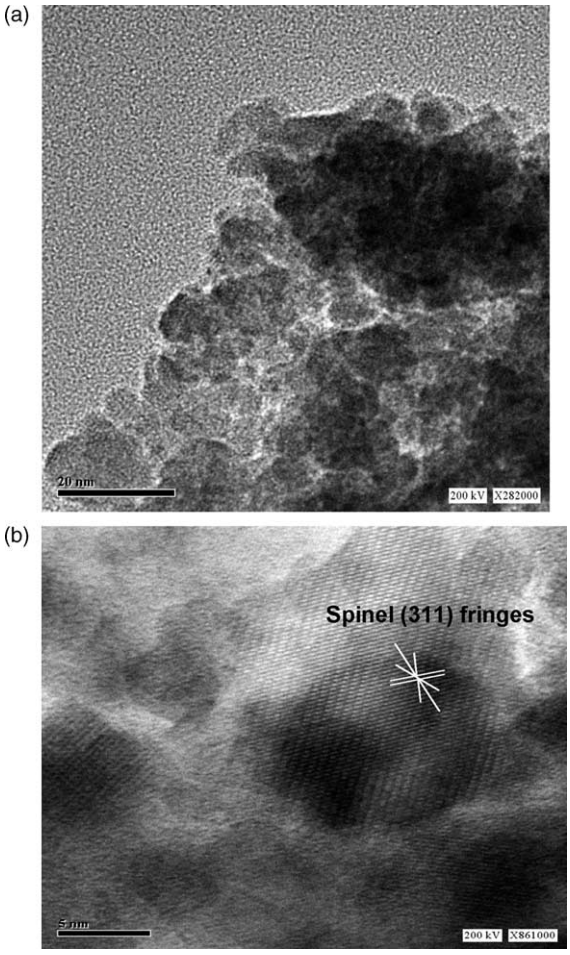

Fig. 2. TEM (a) and HRTEM (b) images of $CuFe_2O_4$ nanoparticles.

measurements, the sample was cooled to 2 K with applied magnetic field and then the measurement of magnetic moments was carried out. Fig. 4(a) shows the ZFC–FC curve of nanocrystalline $CuFe_2O_4$. It can be observed that the ZFC magnetization, the temperature increases from 2 to 350 K, the magnetization values reaches a maximum of 26.45 emu/g at 83 K and starts to decrease with further increasing temperature. The FC magnetization shows the maximum magnetization of 26.9 emu/g at 2 K and steadily decreases with increasing temperature. From the Fig. 4(a), the irreversibility temperature (T_{irr}) and (T_{max}) were measured and the results are given in Table 2. In general, the T_{irr} represents the blocking temperature of particles with highest energy barrier and T_{max} is the average blocking temperature. The difference between T_{max} and T_{irr} corresponds to the width of blocking temperature distribution [26]. Below the blocking temperature, the separation can be observed which may be due to the freezing of disordered surface spins that leads to the glassy state. Under ZFC condition, the FC values are larger than the ZFC value that causes the magnetic nanoparticles reduce its magneto crystalline energy [27]. It is also seen that, below the blocking temperature the non-zero magnetization was observed which is a characteristic features of ferrimagnetic materials [28].

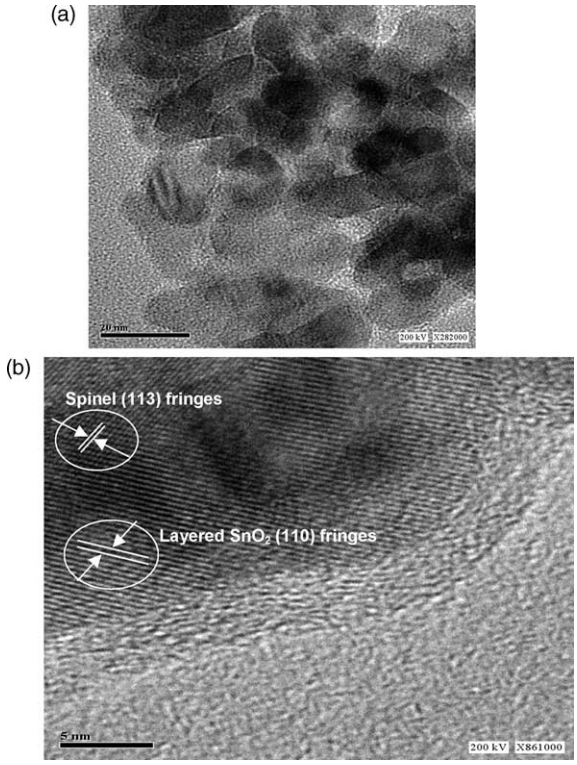

Fig. 3. TEM (a) and HRTEM (b) images of $CuFe_2O_4$/5 wt% SnO_2 nanocomposites.

Fig. 4(b) shows the ZFC and FC curves of $CuFe_2O_4$/1 wt% SnO_2 nanocomposites. In this case, at 2 K the magnetization values are increased when compare with parent $CuFe_2O_4$. It can also be seen that the blocking temperature is decreased with the addition of 1 wt% SnO_2. After the T_B the ZFC and FC curves are superimposed which shows the narrow particle size distribution of the nanoparticles [29]. The saturation magnetization of $CuFe_2O_4$/1 wt% SnO_2 at 2 K is 40.2 emu/g, which is higher than the parent $CuFe_2O_4$ of 26 emu/g. The increase in Ms value may be due to the cation redistribution of inverse $CuFe_2O_4$ structure. Similar type of observations has already done on $NiFe_2O_4$ [30]. Because, Sn^{4+} has strong preference to occupy octahedral sites, hence it may replace some of the Fe^{3+}/Cu^{2+} ions from B-sites to A-sites due to the balancing the ionic distribution of cationic sites. Therefore, the saturation magnetization increases due to the change in magnetic moment of A and B-sites.

Fig. 4(c) shows the ZFC and FC magnetization curve of 5 wt% SnO_2 coated $CuFe_2O_4$ nanoparticles. It is seen that the ZFC and FC curves separated and broad up to 350 K. The saturation magnetization values are decreased as compared to the above two systems which may be due to the magnetic dilution effect and the large percentage of surface spins, with disordered magnetic orientation [31]. Surprisingly, the blocking temperature also not in regular manner, which may be due to the consequence of compositional changes of composites and the critical size of the particles.

The magnetizations of $CuFe_2O_4/xSnO_2$ ($x=0$, 1, 5 wt%) nanocomposites with varying applied field have been studied using SQUID magnetometer at room temperature.

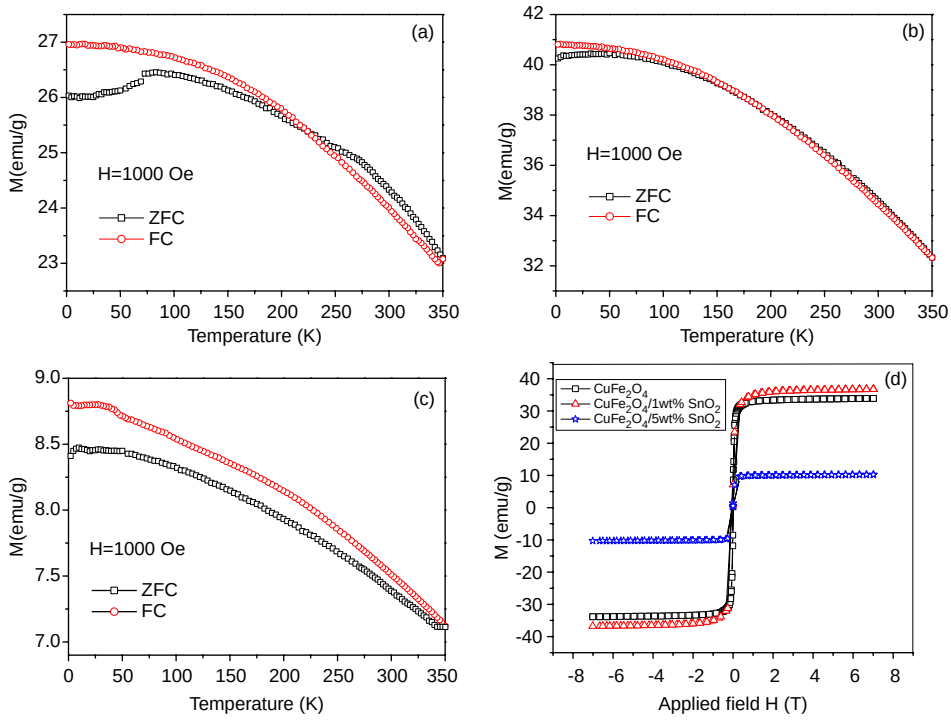

Fig. 4. Dc magnetization behavior of $CuFe_2O_4$ (a), $CuFe_2O_4$/1 wt% SnO_2 (b), $CuFe_2O_4$/5 wt% SnO_2 (c), *M–H* loop (d).

Table 2
SQUID parameters

Sample	SQUID		Ms from hysteresis loop at 300 K (emu/g)	T_{irr} (K)	T_{max} (K)
	Ms from ZFC at 2 K (emu/g)	Ms from ZFC at 350 K (emu/g)			
$CuFe_2O_4$	26	24.3	30	83.3	225
$CuFe_2O_4$ + 1 wt% SnO_2	40.2	34.8	35	50.03	175
$CuFe_2O_4$ + 5 wt% SnO_2	8.4	7.4	11	27.39	350

The magnetic properties of ferrite materials are mainly depending on the particle size, sintering temperature, measuring temperature, milling time, additives, micro structure and external field. Fig. 4(d) shows the ambient temperature *M–H* curve of above said nanocomposites. The *M–H* curve indicates that the particles are superparamagnetic at room temperature with zero coercivity and remanance. It suggests that the thermal energy can overcome the anisotropy energy barrier of a single particle, and the net magnetization of the particle assemblies in the absence of external magnetic field is zero [32]. Table. 2 give the saturation magnetization values of different composites measured at 300 K using SQUID. It can be seen that the SnO_2 addition shows an anomalous behavior. Because the 5% added sample gives the lower saturation magnetization of 11 emu/g. The reduction of Ms value from 30 emu/g for pure $CuFe_2O_4$ is due to the surface effects arising from the non-collinearity of magnetic moments that may be due to the coated SnO_2 is impregnated at the interface of ferrite matrix and pinning of the surface spins [33], which is visualized from the HRTEM images of $CuFe_2O_4/SnO_2$ nanocomposites. And also the increasing particle size as well as the surface disorder with higher concentration of SnO_2 the saturation magnetization values are decreased.

4. Conclusions

Combustion synthesis is found to be a suitable method for preparing nanocrystalline $CuFe_2O_4$ and coated composites. The particle size of copper ferrite is less than 10 nm and the particle size of coated composites is around 20 nm, as evident from TEM and HRTEM images. The X-ray diffraction pattern confirms that $CuFe_2O_4$ possesses tetragonal structure and its composites with cubic structure. The ZFC and FC magnetization curves show the blocking temperature and the ferrimagnetic behavior. The *M–H* curve and temperature dependence magnetization studies confirm that all the studied materials are superparamagnetic in nature at ambient temperature.

Acknowledgements

The authors would like to thank Prof A. Gedanken, Israel for providing TEM and HRTEM analysis. The authors are also

grateful to Prof A.K. Shukla, Director, CECRI for his kind help.

References

[1] M.J. Pitkethly, Mater. Today 7 (2004) 20.
[2] S. Sun, C.B. Murray, L. Folks, A. Moser, Science 287 (2000) 1989.
[3] L. John Berchmans, R. Kalai Selvan, C.O. Augustin, Mater. Lett. 58 (2004) 1928.
[4] C.R. Vestal, Z. John Zhang, Nano Lett. 3 (2003) 1739.
[5] S.J. Stewart, M.J. Tueros, G. Cernicchiaro, R.B. Scorjelli, Solid State Commun. 129 (2004) 347.
[6] L. John Berchmans, R. Kalai Selvan, P.N. Selvakumar, C.O. Augustin, J. Magn. Magn. Mater. 279 (2004) 103.
[7] H. Yahiro, H. Tanaka, Y. Yamamoto, T. Kawai, Solid State Commun. 123 (2002) 535.
[8] C.H. Yan, Z.G. Xu, F.X. Cheng, Z.M. Wang, L.D. Sun, C.S. Liao, J.T. Jia, Solid State Commun. 111 (1999) 287.
[9] Q. Chen, A.J. Rondinone, B.C. Chakoumakos, Z. John Zhang, J. Magn. Magn. Mater. 194 (1999) 1.
[10] X. Huang, Z. Chen, J. Magn. Magn. Mater. 280 (2004) 37.
[11] A.S. Albuquerque, J.D. Ardisson, W.A.A. Macedo, T.S. Plivelic, I.L. Torriani, J. Larrea, E.B. Saitovitch, J. Magn. Magn. Mater. 272–276 (2004) 2211.
[12] X.-H. Huang, Z.-H. Chen, Solid State Commun. 132 (2004) 845.
[13] Z.-H. Yuan, L. de Zhang, J. Mater. Chem. 11 (2001) 1265.
[14] Z.H. Zhou, J.M. Xue, H.S.O. Chan, J. Wang, Mater. Chem. Phys. 75 (2002) 181.
[15] J. Plocek, A. Hutlová, D. Niznanský, J. Burík, J.-L. Rehspringer, Z. Micka, J. Non-Cryst. Solids 315 (2003) 70.
[16] S. Balaji, R. Kalai Selvan, K. Subramanian, S. Angappan, L. John Berchmans, C.O. Augustin, Mater. Sci. Eng., B 89 (2005) 119.
[17] S. Yan, J. Geng, L. Yin, E. Zhou, J. Magn. Magn. Mater. 277 (2004) 84.
[18] H.-W. Wang, S.-C. Kung, J. Magn. Magn. Mater. 270 (2004) 230.
[19] C.O. Augustin, R. Kalai Selvan, R. Nagaraj, L. John Berchmans, Mater. Chem. Phys. 89 (2005) 406.
[20] A. Kale, S. Gubbala, R.D.K. Misra, J. Magn. Magn. Mater. 277 (2004) 350.
[21] M. Sivakumar, A. Gedanken, W. Zhong, Y.W. Du, D. Bhattacharya, Y. Yeshurun, I. Felner, J. Magn. Magn. Mater. 268 (2004) 95.
[22] R. Kalai Selvan, N. Kalaiselvi, C.O. Augustin, C.H. Doh, C. Sanjeeviraja, J. Power Sources (in press).
[23] R. Kalai Selvan, C.O. Augustin, L. John Berchmans, R. Saraswathi, Mater. Res. Bull. 38 (2003) 41.
[24] R. Kalai Selvan, C.O. Augustin, L.C. Sanjeeviraja, V.G. Pol, A. Gedanken, Mater. Chem. Phys. (in press).
[25] C.S. Johnson, N. Li, J.T. Vaughey, S.A. Hackney, M.M. Thackeray, Electrochem. Commun. 7 (2005) 528.
[26] H. Nathani, S. Gubbala, R.D.K. Misra, Mater. Sci. Eng., B 121 (2005) 126.
[27] C. Nethravathi, S. Sen, N. Ravishanker, M. Rajamathi, C. Pietzonka, B. Harbrecht, J. Phys. Chem. B 109 (2005) 11468.
[28] A. Sarkar, S. Kapoor, G. Yashwant, H.G. Salunke, T. Mukherjee, J. Phys. Chem. B 109 (2005) 7203.
[29] J. Lai, K.V.P.M. Shafi, A. Ulman, K. Loos, Y. Lee, T. Vogt, W.-L. Lee, N.P. Ong, J. Phys. Chem. B 109 (2005) 15.
[30] C.N. Chinnasamy, A. Narayanasamy, N. Ponpandian, K. Chattapadhyay, K. Shinoda, B. Jeyadevan, K. Tohji, K. Nakatsuka, T. Furubayashi, I. Nakatani, Phys. Rev. B 63 (2001) 184108.
[31] S.V. Pol, V.G. Pol, A. Frydman, G.V. Churilov, A. Gedanken, J. Phys. Chem. B 109 (2005) 9495.
[32] Y.L. Hou, H. Kondoh, M. Shimojo, K.O. Sako, N Ozaki, T. Kogure, J. Phys. Chem. B 109 (2005) 4845.
[33] S. Si, C. Li, X. Wang, D-Yu., Q. Peng, Y. Li, Cryst Growth Des. 5 (2005) 391.